# Mercury isotope variations in surface soils in different contaminated areas in Guizhou Province, China

FENG XinBin[1*], YIN RunSheng[2], YU Ben[1,3] & DU BuYun[1,3]

[1] State Key Laboratory of Environmental Geochemistry, Institute of Geochemistry, Chinese Academy of Sciences, Guiyang 550002, China;

[2] State Key Laboratory of Ore Deposit Geochemistry, Institute of Geochemistry, Chinese Academy of Sciences, Guiyang 550002, China;

[3] Graduate University of the Chinese Academy of Sciences, Beijing 100039, China

Guizhou Province is known as a heavily Hg-polluted area in China due to its special geochemical background and complicated Hg emission sources. In this study, we investigated the Hg isotope compositions of surface soil samples in the Hg mining area, zinc smelting area, coal combustion area, which are known to be the typical pollution regions of Hg in this province. We also compared the Hg isotopic fingerprints of primary Hg sources, such as hydrothermal Hg-bearing ores, coals and atmospheric Hg samples. According to our study, Hg stored in surface soils in different pollution regions in Guizhou Province displays a wide range of both mass dependent fractionation (MDF, $\delta^{202}$Hg) and mass independent fractionation (MIF, $\Delta^{199}$Hg). $\delta^{202}$Hg varies by 2.0‰ and $\Delta^{199}$Hg varies by 0.25‰ in the investigated surface soils. This study demonstrated that using a "MDF-MIF" two dimensional Hg isotope system could be particularly useful in discriminating Hg sources in soils.

mercury, isotope, surface soil, source tracing

Mercury (Hg) is a globally distributed toxic element. Since the industrialization, the amount of Hg circulating in the atmosphere has roughly tripled [1]. Hg pollution is serious in China, particularly in Guizhou Province, SW China [2]. Guizhou is situated in the Circum-Pacific Global Mercuriferous Belt, is currently one of the most important Hg production base in the world. Although large-scale Hg mining activities were completely stopped in this province since 2004, however, long-terms of Hg mining activities resulted in significant quantities of Hg wastes, which are continuing to impact the local environments [2].

Hg is an important associate element in zinc (Zn) ores [3]. Guizhou is an important center for artisanal Zn smelting. Zn ores produced in Guizhou contain high-Hg concentrations. For instance, Feng and co-workers [4] reported an average HgT of 66.8 μg g$^{-1}$ in sulfide Zn ores from Hezhang, NW Guizhou. Li and co-workers [5] found total Hg content in

Zn concentrates from Guizhou ranged from 1.06 to 87.1 μg g$^{-1}$. As no pollution devices were applied during artisanal zinc smelting, a large quantity of Hg was released to the environment, resulting in serious Hg contamination to the surroundings [4,5].

Guizhou is also known as one of largest coal producer in China. Currently, > 50 million tons of coals were combusted each year for both industrial and domestic purposes, and most coals were used with less or no flue gas controls [6]. Due to the special geochemical background, Hg content in coal from Guizhou is elevated compared to that in other regions in China. Hence, a large quantity of Hg is released during coal combustion, resulting in Hg pollution to the ambient air and the adjacent environment [2,6].

Although Hg contamination status was well documented in Guizhou [2], however, numerous Hg emission sources in this province need to be discriminated so that Hg remediation and environmental policy could be further carried out. The recent growth of Hg isotope studies was facilitated by

*Corresponding author (email: fengxinbin@vip.skleg.cn)

the development of a technique using multi-collector inductively coupled plasma mass spectrometry (MC-ICP-MS) [7]. Fractionation of Hg has been detected in a large variety of environmental compartments, e.g. hydrothermal Hg-bearing ores [8–10], coals [11,12], soil/sediments [7,13–15], atmospheric Hg [16] and biological tissues [17]. Above cited studies have unequivocally demonstrated that variations in the Hg isotopic signature could be used in the future as tracers to distinguish between Hg sources and important chemical transformation processes in the environment.

Soil plays an important role in the global cycling of Hg because it acts both as a sink and a source of Hg to biota, atmosphere and hydrological compartments [18]. In this study, we evaluated the feasibility of employing Hg isotope to track sources of Hg in soils from different contaminated areas in Guizhou, e.g. Hg mining area, power plant and zinc melting areas. Our purpose was to investigate whether soil Hg from different sources have diagnostic Hg isotopic fingerprints.

# 1 Materials and methods

## 1.1 Study areas and sampling

As shown in Figure 1, surface soils samples (0–2 cm) were taken from the four areas in Guizhou Province. (1) Wanshan Mercury Mine (WSMM), located in the eastern part of Guizhou, is known as the "Mercury Capital" in China. Hg mining activities have been documented for more than 3000 years in WSMM [2]. Hg ores had been intensively extracted from WSMM during the past 50 years. Large volumes of Hg-bearing waste rocks and roasted calcines containing Hg residual levels of Hg, have caused serious pollution to soil/sediment, water, and agricultural crops in the surroundings [2]; (2) Hezhang Zn Smelting Area (HZSA) is situated in NW Guizhou, large quantities of artisanal Zn smelting workshops were scattered in this region. The detailed description of Hg pollution in HZSA is described by Feng and his co-workers [4,5]; (3) Qingzhen Power Plant (QZPP) is a large coal fired power plant (300 MW). In QZPP, the soils
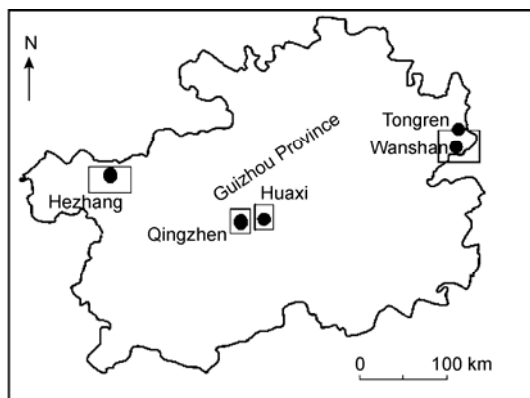


**Figure 1** Study area and sampling site.

were found to contain elevated levels of Hg (> 0.30 μg g$^{-1}$, respectively), which is known to be more associated with coal combustion [19]. (4) Huaxi Control Site (HXCS) was chosen as the control site, HXCS has no direct Hg point contamination source. The concentrations of gaseous element Hg in ambient air (2.12–12.8 ng m$^{-3}$) and total Hg content (HgT) in surface soil (0.25–0.30 μg g$^{-1}$) represent the regional background levels [20].

Surface soil samples from agriculture land including 8 at WSMM, 4 at HZSA, 3 at QZPP, and 3 regarded as reference site in HXCS were collected, respectively. All collected samples were stored in sealed polyethylene bags to avoid any contamination during sampling. In the laboratory, the soil samples were air dried and then homogenized. All the samples were ground to sub-minus 150 mesh (<106 μm) and subsequently sealed in polyethylene bags prior to HgT and Hg isotopic analysis. All the results are expressed on a dry weight basis.

## 1.2 Total mercury analysis

For HgT analysis, ground soil samples (~0.5 g) were placed in a glass tube and then digested in a water bath at 95°C using a fresh mixture of HCl and HNO$_3$ (1:3, v/v) for 30 min. Hg concentrations in all digested solutions were determined using BrCl oxidation and SnCl$_2$ reduction coupled with cold-vapor atomic absorption spectrometry (CVAAS). A certified reference material (CRM BCR 580) was used to accomplish QA/QC, and the HgT recovery for CRM BCR 580 was in the range of 92%–105%, and the relative percentage difference of sample duplicates was < 9%. The results demonstrated that the pretreatment procedures can quantitatively recover Hg from the soil samples.

## 1.3 MC-ICP-MS measurement

Hg isotopic ratios were determined by MC-ICP-MS using a Nu-Plasma mass spectrometer equipped with twelve Faraday cups (Nu Instruments, Great Britain) at the State Key Laboratory of Environmental Geochemistry, Institute of Geochemistry, Chinese Academy of Sciences, China, according to a previous established method [21]. Hg isotopic variations are reported in delta notation in units of per mil (‰) and referenced to the NIST SRM 3133 Hg standard (analysed before and after each sample) and using the following equation:

$$\delta^{xxx}Hg(‰) = \left( \frac{^{xxx}Hg/^{198}Hg_{sample}}{^{xxx}Hg/^{198}Hg_{NISTSRM3133}} \right) - 1 \times 1000. \quad (1)$$

Mass independent fractionation (MIF) of Hg isotopes are calculated using the "capital delta" notation, $\Delta^{xxx}Hg$ (‰), which is defined as the difference between the measured $\delta^{xxx}Hg$ values and the predicted $\delta^{xxx}Hg$ values from MDF, according to the following equations [22]:

$$\Delta^{201}Hg \approx \delta^{201}Hg-(\delta^{202}Hg * 0.752), \qquad (2)$$

$$\Delta^{199}Hg \approx \delta^{199}Hg-(\delta^{202}Hg * 0.252). \qquad (3)$$

Uncertainties reported in this paper correspond to the larger value of the uncertainty of repeated measurements of the same digest (typically $n = 2$) in different analysis sessions. Hg in reference material UM-Almadén was measured the same way as other samples in each analytical session. The overall average and uncertainty of $\delta^{202}Hg$ was $-0.61‰ \pm 0.09‰$ ($2\sigma$, $n = 5$), of $\Delta^{201}Hg$ was $0.02‰ \pm 0.06‰$ ($2\sigma$, $n = 5$) and of $\Delta^{199}Hg$ was $-0.03‰ \pm 0.05‰$ ($2\sigma$, $n = 5$) for all UM-Almadén measurements, which agrees well with data reported in literature [22]. When the calculated $2\sigma$ was smaller than that of the replicate analyses of the UM-Almaden, the uncertainty associated to UM-Almaden was used instead.

Based on the HgT content measured in Section 2.2, all the digested solution were diluted to a final Hg concentration of $2-5$ ng mL$^{-1}$ before MC-ICP-MS analysis. HgT concentrations of digest solutions were also estimated by MC-ICP-MS using $^{202}Hg$ signals. The differences between HgT measured by CVAAS and MC-ICP-MS were $< 13\%$.

## 2   Results and discussions

### 2.1   Total Hg content in surface soils in different pollution areas

Figure 2 shows the results of HgT concentrations in the surface soils in different contaminated areas in Guizhou. HgT in surface soils were highly variable, ranging between 0.13 and 127 µg g$^{-1}$. In WSMM, Hg mining operations severely enhanced the mobilization of Hg through the smelting activities and the depositions of mine tailings and thus resulted in elevated Hg levels in soils. In this study, HgT concentration in surface soils in WSMM are exceptionally high, ranged from 49 to 127 µg g$^{-1}$, with a geomean HgT of 78.48 µg g$^{-1}$ ($n=8$). According to the level III (1.5 µg g$^{-1}$) in the Chinese national standard for soil environmental quality, the contamination level in WSMM is considered non-suitable for e.g. agricultural or residential use [23].

The HgT content in HZSA ranged from 0.23 to 0.37 µg g$^{-1}$, with a geomean value of 0.29 µg g$^{-1}$ (Figure 2). Feng and co-workers [4] demonstrated that the contamination of Hg in surface soils in HZSA is mainly derived from deposition of atmospheric Hg species emitted from artisanal Zn smelting. In general, the HgT in HZSA is much lower than WSMM. However, the surface soils of HZSA are seriously contaminated with Hg compared to the previous established local background HgT ($0.14 \pm 0.05$ µg g$^{-1}$) in HZSA [4].

As shown in Figure 2, the lowest HgT concentrations in surface soils were observed in QZPP. The HgT content in QZPP ranged from 0.13 to 0.18 µg g$^{-1}$, with a geomean value of 0.15 µg g$^{-1}$, which was similar to the level I (0.15 µg g$^{-1}$) in the Chinese national standard for soil environmental quality [23]. However, it is interesting to notice that, at the HXCS reference site, the geomean HgT in surface soil is 0.29 µg g$^{-1}$ ($n =3$), which is elevated compared to that in QZPP. Compared to the background Hg concentrations recorded in remote pristine areas, the HgT level in HXCS is significantly elevated [24]. The elevated HgT in HXCS may be derived from geological sources and/or contaminated by anthropogenic activities.
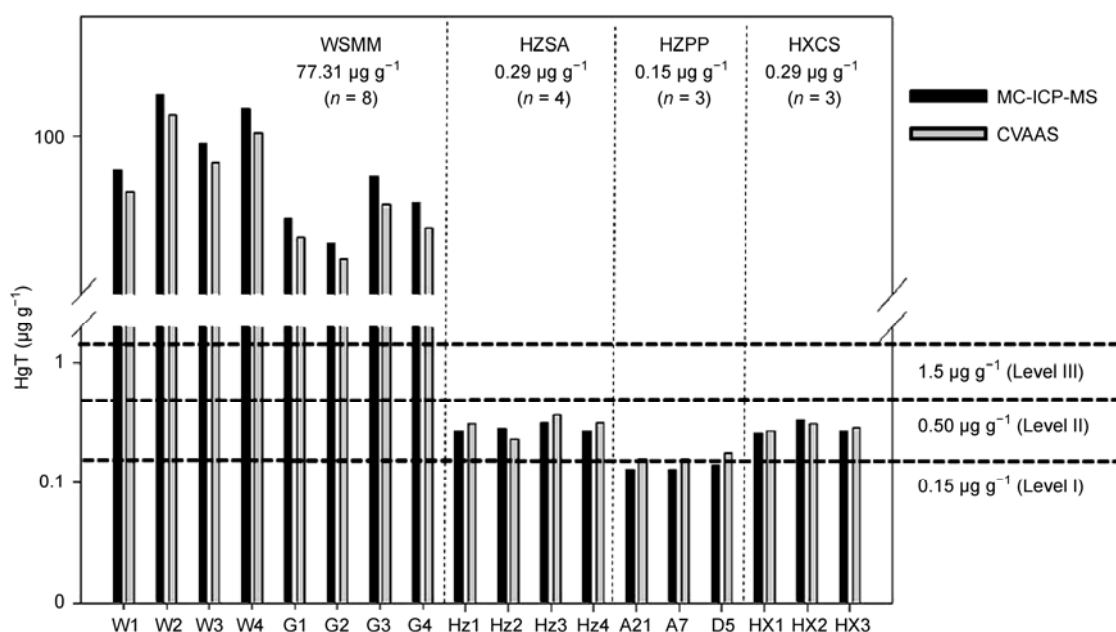


**Figure 2**   Total Hg distribution in surface soil samples collected from Guizhou Province.

## 2.2   Comparation of Hg isotope composition in different Hg sources in the environment

Anthropogenic Hg originates primarily from metallurgical process of hydrothermal ore samples (e.g. cinnabar, meta-cinnabar, or Hg-bearing ores) and the combustion of fossil fuels during a variety of industrial production. Based on data available in Hg isotope literatures, Figure 3 was constructed to illustrate the distinct isotope fingerprints of Hg isotopes in both MDF ($\delta^{202}$Hg) and MIF ($\Delta^{199}$Hg) for the primary Hg sources in the environment. According to Figure 3, although large variations of $\delta^{202}$Hg (>6‰) were observed for hydrothermal Hg sources e.g. cinnabar, meta-cinnabar and sphalerite [8–10,13,14,25–28], it seems that most of hydrothermal Hg-bearing ore samples had $\delta^{202}$Hg values of −0.67‰ ± 0.81‰ (2$\sigma$, *n* =177), with no evidence of significant MIF as shown in Figure 3. For instance, Hintelmann and Lu [8] investigated the Hg isotope composition of cinnabar samples collected from several Hg deposits worldwide, they reported Hg mine has mean $\delta^{202}$Hg of −0.88‰ ± 0.44‰ (2$\sigma$, *n* =14), with ranging from −1.33‰ to 0‰. Smith and co-workers [10] investigated the isotopic composition of Hg in rocks, ore deposits, and active spring deposits from the California Coast Ranges. They demonstrated a mean $\delta^{202}$Hg of −0.64‰ ± 0.87‰ (2$\sigma$, *n* =146) in all investigated samples. Blum and Bergquist [22] measured the cinnabar samples from the world's largest Hg mine, and they demonstrated a $\delta^{202}$Hg value of −0.54‰. Yin and co-workers [28] investigated the Hg isotope composition of unroasted Hg ores in WSMM, and they reported a similar $\delta^{202}$Hg of −0.74‰ ± 0.11‰, (2$\sigma$, *n* = 14) the unroasted Hg ores. Sonke and co-workers [26] investigated the isotopic compositions of several sphalerite samples which showed similar $\delta^{202}$Hg of −0.24‰ ± 0.15 ‰ (2$\sigma$, *n* = 2). Above data fall within the range of most hydrothermal ore deposits as shown in Figure 3.

As shown in Figure 3, the Hg isotope signature in coal samples showed a different pattern compared to hydrothermal Hg samples [11,12]. The $\delta^{202}$Hg of coal ranged from −0.11‰ to −2.98‰, with a mean value of −1.29‰ ± 0.64‰ (2$\sigma$, *n* =146), which is slightly smaller compared to hydrothermal ore samples. However, coal samples showed detectable MIF of −0.09‰ ± 0.17‰ (2$\sigma$, *n* =146). Hg isotopic signatures of coal deposits are the product of the Hg isotopic composition of atmospheric and fluvial inputs to the initial coal-forming environment with possible additions of Hg from subsurface fluids and possible losses during subsequent diagenesis [12]. Coal formations from the U.S., China, and Russia-Kazakhstan revealed a range of $\Delta^{199}$Hg and $\Delta^{201}$Hg anomalies in a near 1:1 proportions between +0.38‰ and −0.66‰ [11]. Such a 1:1 ratio was observed during Hg$^{II}$ photochemical reduction experiments [17] and suggests that much of the Hg in the coals has been undergone photo-reduction prior deposited to coals [11].

According to refs. [16,29], Hg entering the environment through varies industrial activities probably have little to no MIF signatures. However, large variation of MIF was observed in the sub-surface environment compartments such as in aquatic systems [17] and atmospheres [16]. The negative MIF of Hg in the atmospheric samples is inspiring because elemental Hg$^{0}$ has an extended tropospheric residence time entailing global-scale transportation and interhemispherical boundary-layer mixing ratio homogeneities [30,31]. Hg could undergo many geochemical processes during its cycling before being stored into different reservoirs, such as continental soils. Fractionation of Hg isotopes is demonstrated to be occurred through multiple biophysico-chemical processes, e.g. microbial reduction [32], photo-reduction [17] and volatilization [33], etc. Hence, the isotope composition of Hg in atmosphere can be altered
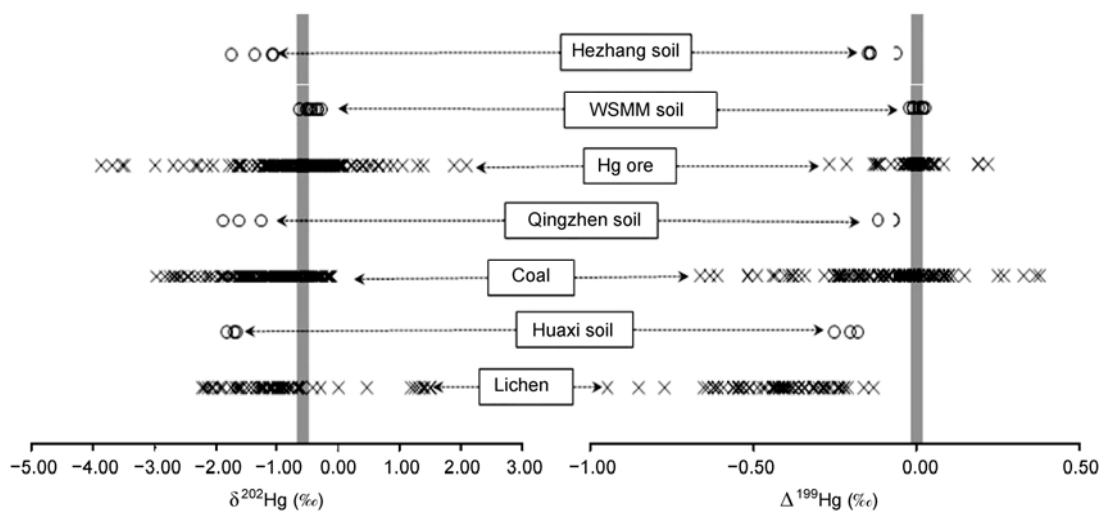


**Figure 3**   Comparison of $\delta^{202}$Hg (‰) and $\Delta^{199}$Hg(‰) values in Guizhou soils. Selected literature data on Hg isotopic compositions in different Hg sources [8–14,25–28] is also included.

through global and regional cycling of Hg, after Hg is emitted from natural sources and anthropogenic sources. Epiphytic lichens have been used as surrogates for decades in reflecting atmospheric wet/dry Hg deposition [16]. As shown in Figure 3, most lichen samples that obtained Hg after it had been through cycling in the environment have $\Delta^{199}$Hg values ($-0.43‰ \pm 0.14‰$, $2\sigma$, $n$=72) significantly different from hydrothermal Hg-bearing ores and coal samples. Recently, Sonke [29] conducted a global model of MIF of Hg isotopes on the earth environment. This model demonstrated that Hg MIF is a common phenomenon at the global scale and photo-reduction of aqueous Hg is the main MIF inducing process results in negative atmospheric $\Delta^{199}$Hg.

## 2.3   Hg isotope composition in Guizhou soils

Figure 4 shows a three-isotope plot of $\Delta^{199}$Hg Hg vs $\delta^{202}$Hg for all surface soils (this study), coal samples from Guiyang [19], Hg ore and Hg waste samples collected from WSMM [14,28]. The isotope data in QZPP ($n$ =3) are already published in ref. [14], here we added them to Figure 4 for comparison. We observed a ~2.0‰ range in $\delta^{202}$Hg values (MDF) and a detectable MIF (range of ~0.25‰) in $\Delta^{199}$Hg values among all investigated samples as shown in Figure 4. The external reproducibility [$2\sigma$] of this method is 0.08‰ for $\delta^{202}$Hg and 0.05‰ for $\Delta^{199}$Hg. This graph revealed distinct Hg isotope signatures in soils collected from different Hg polluted areas, illustrating that Hg isotopic compositions could be useful in tracing Hg in soils from different contaminated sources.

Hg isotope composition of cinnabar ($\delta^{202}$Hg= $-0.74‰ \pm 0.11‰$, $2\sigma$, $n$ = 14) and calcine ($\delta^{202}$Hg= $0.08‰ \pm 0.20‰$, $2\sigma$, $n$ = 11) in WSMM were investigated by Yin and

co-workers [28], implying that significant ( $P< 0.05$, $t$-test) Hg MDF of ~0.8‰ occurred during the Hg retorting process. As shown in Figure 4, the $\delta^{202}$Hg values of WSMM soils ($-0.43‰ \pm 0.12‰$, $2\sigma$, $n = 8$) fall in between Hg ore and Hg waste calcines in WSMM, which implies Hg in WSMM soils are primarily originates from a mixing of Hg ore and Hg waste calcines. MIF in $\Delta^{199}$Hg values in WSMM soils ranged from $-0.02‰$ to $0.07‰$, which were statistically insignificant ($P > 0.20$, $t$-test). So far, the major processes known to induce MIF are photo-reactions of aqueous $Hg^{II}$ phases and Me-Hg photo-degradation, which lead to enrichment of the odd isotopes in the residual $Hg^{II}$ and Me-Hg pool [17]. Although photo-reduction of aqueous Hg phases may induce MIF in the soil solution, considering the large Hg pool (with HgT ranged from 49 to 127 $\mu g\ g^{-1}$) in soils and that photochemical processes will most plausibly only affect a tiny fraction of the pool, a detectable MIF in WSMM soils would not be expected.

Different with surface soils collected from WSMM, the Hg stored in soils from other areas, including HZSA, QZPP and HXCS are characterized with much lower $\delta^{202}$Hg values and detectable negative MIF ($\Delta^{199}$Hg<0) as shown in Figure 4. (1) The Hg stored in SS from the HZSA is characterized by $\delta^{202}$Hg values ranging from $-1.06‰$ to $-1.75‰$ (Mean: $-1.32‰ \pm 0.32‰$, $2\sigma$, $n = 4$) and $\Delta^{199}$Hg values ranging from $-0.06‰$ to $-0.15‰$ (Mean: $-0.12‰ \pm 0.04‰$, $2\sigma$, $n = 4$); (2) the Hg stored in SS from the QZPP is characterized by $\delta^{202}$Hg values ranging from $-1.26‰$ to $-1.88‰$ (Mean: $-1.59‰ \pm 0.31‰$, $2\sigma$, $n = 3$) and $\Delta^{199}$Hg values ranging from $-0.07‰$ to $-0.12‰$ (Mean: $-0.09‰ \pm 0.03‰$, $2\sigma$, $n = 3$); (3) the Hg stored in SS from the HXCS is characterized by $\delta^{202}$Hg values ranging from $-1.66‰$ to $-1.82‰$ (Mean: $-1.73‰ \pm 0.08‰$, $2\sigma$, $n = 3$) and $\Delta^{199}$Hg values ranging from $-0.18‰$ to $-0.25‰$ (Mean: $-0.21‰ \pm 0.04‰$, $2\sigma$, $n = 3$). As mentioned in Section 2.2, it is demonstrated hydrothermal ore samples, e.g. cinnabar, meta-cinnabar and sphalerite, generally have no evidence of significant MIF as shown in Figure 3. According to Biswas and co-workers [11], two coal samples from Guiyang basin did not show MIF. Perhaps, the variations in MDF and MIF certainly reflect the fact that the soil Hg reservoir is a mixture of different sources and the result of various physicochemical reactions.

Surface soils generally contain organic matter, which can be assumed to function like a filter, retaining most though not all of the Hg brought to the soil through dry and wet depositions [1]. Atmospheric Hg deposition could be an important source of Hg in surface soils from continental compartments [11,29]. Hg MIF is generally understood to be caused by the nuclear volume effect [34] and/or the magnetic isotope effects [35]. Previous studies demonstrated that Hg MIF is caused by photochemical reduction of $Hg^{II}$ and Me-Hg to $Hg^{0}$ [17]. When $\Delta^{199}$Hg vs $\Delta^{201}$Hg is plotted for each of these photochemical reduction processes a slope of 1.36 is observed for methyl-Hg and 1.00 for $Hg^{II}$
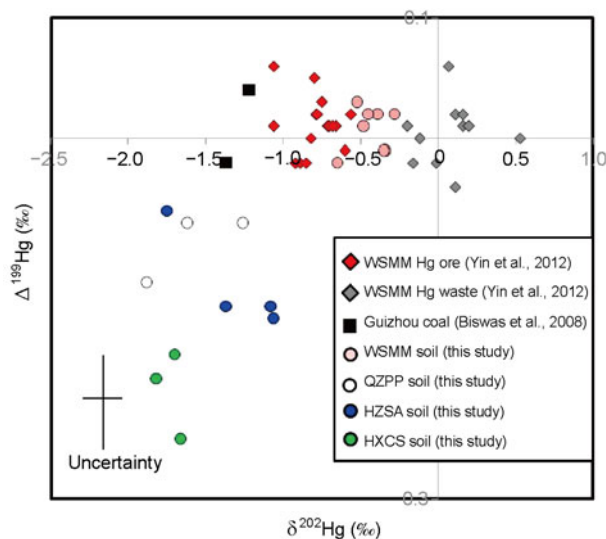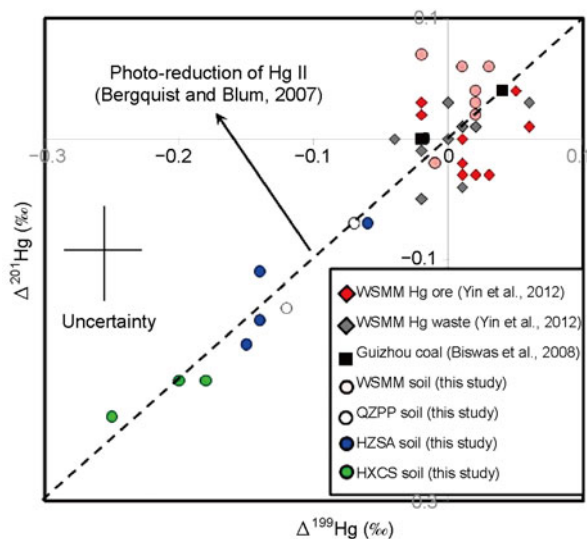


**Figure 4**   Three-isotope plot of $\Delta^{199}$Hg vs $\delta^{202}$Hg for Guizhou soils, coal samples from Guiyang [11], Hg ore and Hg waste samples collected from WSMM [14,28].

**Figure 5** Three-isotope plot of $\Delta^{199}$Hg Hg vs $\Delta^{201}$Hg for Guizhou soils, coal samples from Guiyang [11], Hg ore and Hg waste samples collected from WSMM [14,28].

photo-reduction, though more experiments have indicated that photo-reduction of Hg-NOM species (Hg bound to natural organic matter) can produce slopes ranging from 1.19 to 1.31 [17]. As shown in Figure 5, we observed a ratio of ~1 between $\Delta^{201}$Hg and $\Delta^{199}$Hg in soil samples collected from HZSA, QZPP and HXCS. This ratio is similar to that observed during photo-reduction of Hg$^{II}$, indicating that part of Hg in soil in these regions could undergo photo-reduction process before being deposited to the soils.

Recent studies of direct and indirect air samples (e.g. moss and lichens) showed strong evidence of negative MIF ($\Delta^{199}$Hg = –0.43‰ ± 0.14‰, 2$\sigma$, n = 72) as shown in Figure 3. The negative $\Delta^{199}$Hg signature in atmospheric Hg samples is perhaps due to the photo-reduction of aqueous Hg [27]. The Hg stored in soil samples collected from HZSA, QZPP and HXCS, generally have much lower HgT values compared to that in WSMM (Figure 2). This further suggests that atmospheric Hg deposition could be an important source of Hg in the soils from HZSA, QZPP and HXCS. Indeed, MIF varies in different Hg contaminated areas. Our study agreed well with previous studies, for instance, organic forest soils collected at remote sites in the continental United States in New Hampshire, Wyoming, and Washington and in the Maya Mountains of Belize were characterized by $\delta^{202}$Hg values ranging from –1.0‰ to –1.8‰ (–1.37‰ ± 0.30‰, 2$\sigma$, n = 10) and $\Delta^{199}$Hg values ranging from 0.0 to –0.4‰ (–0.20‰ ± 0.11‰, 2$\sigma$, n = 10). The atmospheric origin of Hg is assumed to be one of the dominated sources in those areas [11].

## 3   Conclusions

In this study, we evaluated the feasibility of using Hg isotope composition as a tool to trace Hg contamination sources in surface soils. This research suggests that combined MDF and MIF Hg isotope signatures can be used to identify and trace Hg pollution in the soil compartment. The MIF signatures of Hg sources could be particularly diagnostic in apportioning Hg inputs in locations impacted by multiple identifiable local and regional Hg sources.

1 Lindqvist O, Johansson K, Aastrup M, et al. Mercury in the Swedish environment. Water Air Soil Pollut, 1991, 55: 193–216

2 Feng X B, Qiu G L. Mercury pollution in Guizhou, Southwestern China — An overview. Sci Total Environ, 2008, 400: 227–237

3 Yin R, Feng X, Li Z, et al. Metallogeny and environmental impact of Hg in Zn deposites in China. Appl Geochem, 2012, 27: 151–160

4 Feng X, Li G, Qiu G. A preliminary study on mercury contamination to the environment from artisanal zinc smelting using indigenous methods in Hezhang county, Guizhou, China: Part 2. Mercury contaminations to soil and crop. Sci Total Environ, 2006, 368: 47–55

5 Li G, Feng X, Qiu G, et al. Environmental mercury contamination of an artisanal zinc smelting area in Weining County, Guizhou, China. Environ Pollut, 2008, 154: 21–31

6 Streets D, Hao J, Wu Y, et al. Anthropogenic mercury emissions in China. Atmos Environ, 2005, 39: 7789–7806

7 Foucher D, Hintelmann H. High-precision measurement of mercury isotope ratios in sediments using cold-vapor generation multi-collector inductively coupled plasma mass spectrometry. Anal Bioanal Chem, 2006, 384: 1470–1478

8 Hintelmann H, Lu S Y. High precision isotope ratio measurements of mercury isotopes in cinnabar ores using multi-collector inductively coupled plasma mass spectrometry. Analyst, 2003, 128: 635–639

9 Smith C N, Kesler S E, Klaue B, et al. Mercury isotope fractionation in fossil hydrothermal systems. Geology, 2005, 33: 825–828

10 Smith C N, Keslera S E, Blum J D, et al. Isotope geochemistry of mercury in source rocks, mineral deposits and spring deposits of the California Coast Ranges, USA. Earth Planet Sci Lett, 2008, 269: 399–407

11 Biswas A, Blum J D, Bergquist B A, et al. Natural mercury isotope variation in coal deposits and organic soils. Environ Sci Technol, 2008, 42: 8303–8309

12 Lefticariu L, Blum J, Gleason J. Mercury isotopic evidence for multiple mercury sources in coal from the Illinois Basin. Environ Sci Technol, 2011, 45: 1724–1729

13 Foucher D, Ogring N, Hintelmann H. Tracing mercury contamination from the Idrija Mining Region (Slovenia) to the Gulf of Trieste using Hg isotope ratio measurements. Environ Sci Technol, 2009, 43: 33–39

14 Feng X, Foucher D, Hintelmann H, et al. Tracing mercury contamination sources in sediments using mercury isotope compositions. Environ Sci Technol, 2010, 44: 3363–3368

15 Liu J, Feng X, Yin R, et al. Mercury distributions and mercury isotope signatures in sediments of Dongjiang River, the Pearl River Delta, China. Chem Geol, 2011, 287: 81–89

16 Carignan J, Estrade N, Sonke J, et al. Odd isotope deficits in atmospheric Hg measured in lichens. Environ Sci Technol, 2009, 43: 5660–5664

17 Bergquist B A, Blum J D. Mass-dependent and -independent fractionation of Hg Isotopes by photoreduction in aquatic systems. Science, 2007, 318: 417–420

18 Davidson C M, Reis A T, Rodrigues S M, et al. Extractability and mobility of mercury from agricultural soils surrounding industrial and mining contaminated areas. Chemosphere, 2010, 81: 1369–1377

19 Zhang H, Feng X, Larssen T, et al. In inland China, rice, rather than fish is the major pathway for methylmercury exposure. Environ Health Perspect, 2010, 118: 1183–1188

20  Meng B, Feng X, Qiu G, et al. Distribution patterns of inorganic mercury and methylmercury in tissues of rice (*Oryza sativa* L.) plants and possible bioaccumulation pathways. J Agric Food Chem, 2010, 58: 4951–4958

21  Yin R S, Feng X B, Foucher D, et al. High precision determination of mercury isotope ratios using online mercury vapor generation system coupled with multicollector inductively coupled plasma-mass spectrometer. Chin J Anal Chem, 2011, 38, 7: 929–934

22  Blum J D, Bergquist B A. Reporting of variations in the natural isotopic composition of mercury. Anal Bioanal Chem, 2007, 388: 353–359

23  China National Environmental Protection Agency. Environmental Quality Standard for Soils (in Chinese). GB15618–1995, 1995

24  Zhang X M, Luo K L, Sun X Z, et al. Mercury in the topsoil and dust of Beijing City. Sci Total Environ, 2006, 368: 713–722

25  Stetson S J, Gray J, Wanty R B, et al. Isotopic variability of mercury in ore, mine-waste calcine, and leachates of mine-waste calcine from areas mined for mercury. Environ Sci Technol, 2009, 43: 7331–7336

26  Sonke J E, Schafer J, Chmeleff J, et al. Sedimentary mercury stable isotope records of atmospheric and riverine pollution from two major European heavy metal refineries. Chem Geol, 2010, 279: 90–100

27  Gehrke G E, Blum J D, Marvin-DiPasquale M. Sources of mercury to San Francisco Bay surface sediment as revealed by mercury stable isotopes. Geochim Cosmochim Acta, 2011, 75: 691–705

28  Yin R S, Feng X B, Wang J X, et al. Mercury speciation, mercury isotope fractionation during ore roasting process and their implication to source identification of downstream sediments in Wanshan mercury mining area, SW China. Chem Geol, 2012, doi: 10.1016/j.chemgeo.2012.04.030

29  Sonke J E. A global model of mass independent mercury stable isotope fractionation. Geochim Cosmochim Acta, 2011, 75: 4577–4590

30  Yin R, Feng X, Shi W. Application of the stable-isotope system to the study of sources and fate of Hg in the environment: A review. Appl Geochem, 2011, 25: 1467–1477

31  Johansson K, Bergback B, Tyler G. Impact of atmospheric long range transport of lead, mercury and cadmium on the Swedish forest environment. Water Air Soil Pollut Focus, 2001, 1: 279–297

32  Kritee K, Barkay T, Blum J D. Mass dependent stable isotope fractionation of mercury during mer mediated microbial degradation of monomethylmercury. Geochim Cosmochim Acta, 2009, 73: 1285–1296

33  Zheng W, Foucher D, Hintelmann H. Mercury isotope fractionation during volatilization of Hg(0) from solution into the gas phase. J Anal At Spectrom, 2007, 22: 1097–1104

34  Schauble E A. Role of nuclear volume in driving equilibrium stable isotope fractionation of mercury, thallium, and other very heavy elements. Geochim Cosmochim Acta, 2007, 71: 2170–2189

35  Buchachenko A L, Ivanov V L, Roznyatovskii V A, et al. Magnetic isotope effect for mercury nuclei in photolysis of bis (*p*-trifluoromethylbenzyl)mercury. Dokl Phys Chem, 2007, 413: 39–41